Fuel Processing Technology 129 (2015) 24–38

Contents lists available at ScienceDirect

Fuel Processing Technology

journal homepage: www.elsevier.com/locate/fuproc

Catalytic pyrolysis of *Eremurus spectabilis* for bio-oil production in a fixed-bed reactor: Effects of pyrolysis parameters on product yields and character

Tevfik Aysu *

Yuzuncu Yil University, Faculty of Education, Department of Chemistry, 65080, Van, Turkey

ARTICLE INFO

Article history:
Received 29 June 2014
Received in revised form 12 August 2014
Accepted 16 August 2014
Available online xxxx

Keywords:
Energy
Biomass
Pyrolysis
Biofuel
Eremurus spectabilis

ABSTRACT

Conventional slow pyrolysis of *Eremurus spectabilis* samples has been performed in a fixed-bed tubular reactor with (tincal, colemanite and ulexite) and without catalyst in the temperature range between 350 and 550 °C with heating rates of 10, 30, 50 °C/min. The yields of bio-char, bio-oil and gas produced, as well as the compositions of the resulting bio-oils were determined by elemental analysis, Fourier transform infrared spectroscopy (FT-IR) and gas chromatography/mass spectrometry (GC–MS). The effects of pyrolysis parameters such as heating rate, temperature, catalyst type, sweeping gas flow rate and particle size (Dp) on product yields were investigated. The results show that temperature and catalyst are the main factors that effect the conversion of *E. spectabilis* into solid, liquid and gaseous products. The highest liquid yield of 38.14% including aqueous phase was achieved with ulexite catalyst at 500 °C temperature at a heating rate of 50 °C/min when 0.224 > Dp > 0.150 mm particle size raw material and 100 mL/min of sweeping gas flow rate were used. Ninety-one and ninety-seven different compounds have been identified by GC–MS in bio-oils obtained at 350 and 550 °C respectively.

1. Introduction

Today, developing countries including Turkey provide most of their energy requirements from petroleum-based products. The declining of fossil fuel reserves, increasing emissions of greenhouse gases and pollutants, and fluctuating prices of conventional fuels have led scientists to search for clean and renewable substitutes for petroleum-related fuels. In this regard, biomass seems to be one of the most promising sources for production of economical and competitive liquid bio-fuels [1–3]. It has received considerable attention as a cheap, environmentally friendly, renewable and sustainable feedstock in recent years. Besides, using liquid bio-fuels obtained from biomass for heat and power mitigates the release of greenhouse gas emissions as CO_2 released from biomass will be recycled into the plants by photosynthesis [4]. Biomass can be converted into energy in a number of ways: direct combustion processes, thermochemical processes, biochemical processes and agrochemical processes. Thermochemical conversion processes include three subcategories: pyrolysis, gasification, and liquefaction. Pyrolysis is widely recognized as a promising technology for bio-oil and bio-char production. Pyrolysis is the process that converts the biomass into non-condensable gases, charcoal and liquid [5,6].

Bio-oils obtained from pyrolysis of biomass are dark brown mixtures of organic compounds including acids, alcohols, aldehydes, esters, ketones, sugars, phenols, guaiacols, syringols, furans and phenols. They have higher heating values than that of raw materials and can be easily transported and stored. They have the potential for substitution of fuel-oils and can be used to generate heat and electricity or to produce value added chemicals. However, they have lower quality compared to fossil fuels and cannot be mixed with them as they contain high amounts of oxygen ranging between 35 and 45 wt.%. Consequently, they cannot be used directly in conventional gasoline or diesel engines [7]. There are other disadvantages of bio-oils such high water content (15–30 wt.%), acidity coming from formic and acetic acids, high viscosity varying in a large range and presence of ash higher than 0.1 wt.%. In order to improve the quality of bio-oils, several upgrading processes including hydrodeoxygenation, catalytic cracking, emulsification, and steam reforming are required to reduce oxygen content and viscosity and to increase volatility and thermal stability. Steam reforming of bio-oil has the purpose of converting bio-oil in a hydrogen-rich stream [8].

Among the upgrading techniques of bio-oils, catalytic cracking has been used widely as a convenient method by many researchers. Oxygen containing bio-oils are catalytically decomposed to hydrocarbons with the removal of oxygen as H_2O, CO_2 or CO [9]. Nokkosmaki et al. [10] proved ZnO to be a mild catalyst on the composition and stability of bio-oils in the conversion of pyrolysis vapors, and the liquid yields were not found to be substantially reduced. Although it had no effect on the water insoluble fraction (lignin derived), it decomposed the diethyl insoluble fraction (water soluble anhydrosugars and polysaccharides). They found that the viscosity of treated bio-oil with ZnO was decreased

* Tel.: +90 432 225 17 02; fax: +90 432 225 13 69.
E-mail address: tevfikaysu@yyu.edu.tr.

http://dx.doi.org/10.1016/j.fuproc.2014.08.014
0378-3820/

Table 1
Main characteristics of the *Eremurus spectabilis*.

Components	
Moisture (%)	5.6
Proximate analysis[a] *(%)*	
Ash	4.6
Lignin	30.1
Cellulose	38.5
Hemicellulose	20.5
Holocellulose	59.0
Soxhlet extractives (40–60 °C petroleum ether)	0.7
Ultimate analysis[b] *(%)*	
Carbon	39.27
Hydrogen	6.54
Nitrogen	1.28
Oxygen[c]	52.91
H/C molar ratio	1.998
O/C molar ratio	1.010
Empirical formula	$CH_{1.998}N_{0.0279}O_{1.010}$
Higher heating value (MJ/kg)	
Dulong's formula	13.17

[a] Weight percentage on dry basis.
[b] Weight percentage on dry and ash free basis.
[c] By difference.

and the stability of bio-oil was improved. Tekin et al. [11] carried out the hydrothermal liquefaction of beech wood using a natural calcium borate mineral, colemanite at 250, 300 and 350 °C. The highest light bio-oil yield (11.1 wt.%) and the highest heavy bio-oil yield (29.8 wt.%) were obtained at 300 °C with colemanite. The highest heating values were obtained from the hydrothermal liquefaction of biomass using colemanite at 350 °C: 23.81 MJ/kg for light bio-oil and 27.53 MJ/kg for heavy bio-oil. Most of the identified compounds in the light bio-oils were phenols. The heavy bio-oils from the runs both without and with colemanite were composed of phenols, aldehydes, ketones, acids, and benzene derivatives. In a recent study [12], conventional pyrolysis of Niger seed was investigated in a semi batch reactor with and without the presence of catalyst (Al_2O_3, CaO, Kaolin). Thermal pyrolysis yielded maximum 34.5% of oil (by weight basis) at 550 °C temperature. The yield and fuel properties of thermal and catalytic pyrolytic oils were compared. It was found that the presence of catalysts decreased the oil yield marginally whereas it enhanced the fuel properties compared with thermal pyrolysis.

Biomass resources including energy crops, agricultural and forest residues, food and fiber processing residues, and urban residues have been utilized for bioenergy in recent years. Turkey has a great potential of agricultural resources with diverse crops production in 25 million hectares of arable land. There are approximately ten thousand different plants which grow in the lands of Turkey. Many of these plants grow naturally in rural areas and go dormant without using for any purpose [13]. *Eremurus spectabilis*, commonly named as "foxtail lily," is one of the them which is a hardy perennial plant growing to 1 m. *Eremurus* is a genus of nearly 50 species in the family of Liliaceae. Natural populations of this genus are widely distributed on dry and stony grazed hillsides native to the Central Asia and Middle East, including Afghanistan, Iran, Tajikistan, Lebanon and Turkey. Two of *Eremurus* species, namely *E. spectabilis* and *Eremurus cappadocicus* naturally grow in Turkey. *E. spectabilis* is widely distributed in the provinces of Turkey such as Erzurum, Sivas, Yozgat, Bitlis, Usak, Kars, Agri, Erzincan, Van, Artvin and Ardahan [14–18].

In the present study, the conventional pyrolysis of *E. spectabilis* was conducted at five different temperatures between 350 and 550 °C without and with three different boron minerals as catalyst. The catalysts used in this study were tincal ($Na_2B_4O_7 \cdot 10H_2O$), colemanite ($CaB_3O_4(OH)_3 \cdot H_2O$) and ulexite ($NaCaB_5O_6(OH)_6 \cdot 5(H_2O)$) minerals of boron. Effects of pyrolysis parameters such as heating rate, temperature, catalyst type, sweeping gas flow rate and particle size were investigated. However, the main aim of the study was to investigate the effect of catalysts on product yields and to improve the fuel properties of bio-oils with the use of catalyst. Accordingly, characterization and comparison of the bio-oils and bio-chars obtained from pyrolysis were performed with elemental analysis, fourier transform infrared spectroscopy (FT-IR) and gas chromatography/mass spectrometry (GC–MS).

2. Materials and methods

2.1. Materials

E. spectabilis samples, which naturally grow in East Anatolia, were collected from Van region (geographical coordinates: 38° 29′ 39″ North, 43° 22′ 48″ East) in Turkey, in April 2013. They have been dried in open air and ground in Perten Instruments LM120 mill to pass through a screen of 0.425 mm aperture. It was then extracted with petroleum ether (b.p. 40–60 °C) in a Soxhlet extractor for 6 h to find the amount of extractives such as fatty acids, terpenoids and phenolics. Samples of different particle size ranging between 0.150 and 0.850 mm were used to in this study.

Before pyrolysis experiments, ultimate and proximate analysis of the *E. spectabilis* were performed to determine the compositon and evaluate the potential for production of biofuel. Ultimate analysis of the sample was performed using an elemental analyzer (LECO CHNS-932). The tests for determining the main characteristics of the *E. spectabilis* were performed according to Tappi Test methods [19]. Lignin was determined according to Tappi T222. Hollocellulose and cellulose contents were determined using the chloride method [20] and Tappi T202 method. Ash and moisture contents were determined by Tappi T211 and Tappi T264 respectively. Higher heating value (HHV) was calculated

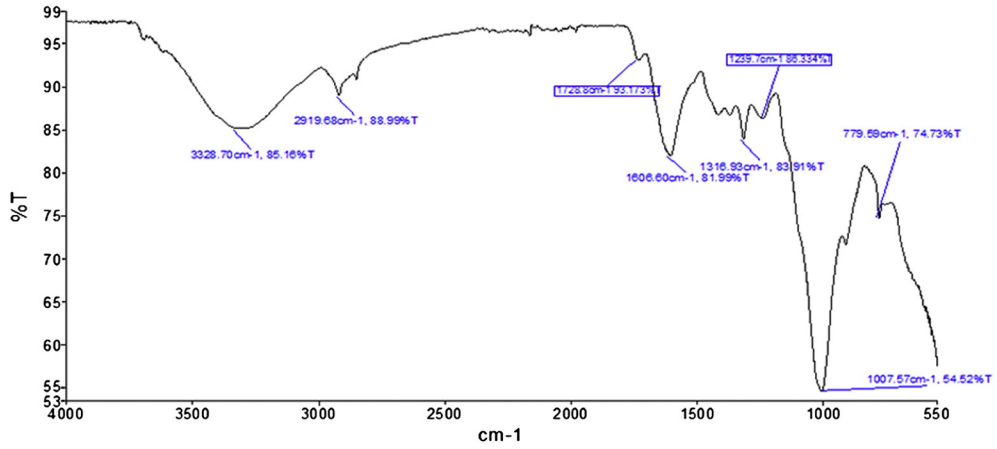

Fig. 1. FT-IR spectra of raw material (*Eremurus spectabilis*).

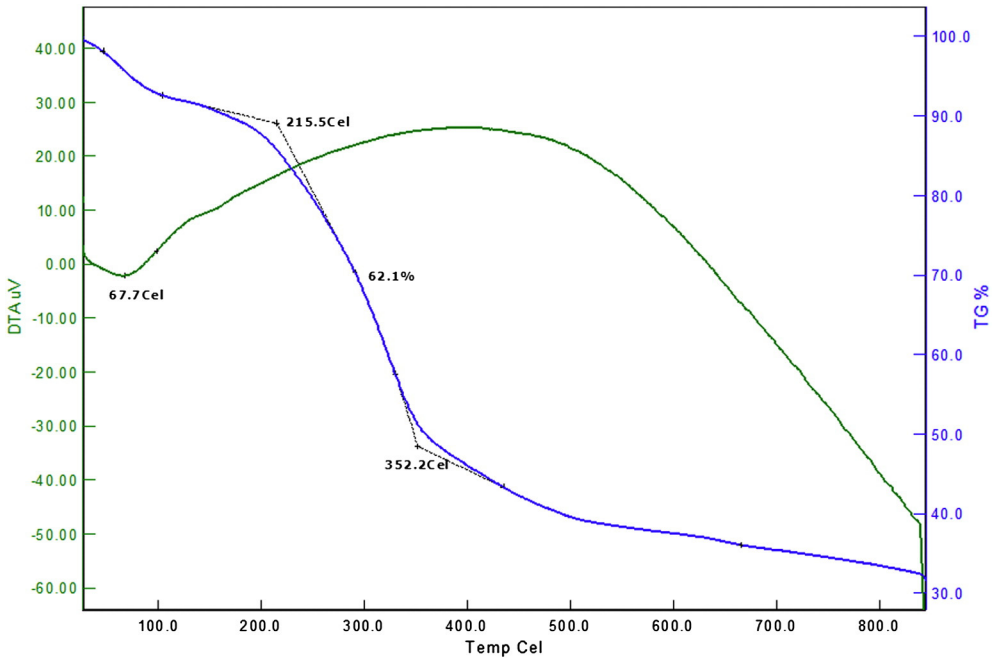

Fig. 2. TG-DTA curves of *Eremurus spectabilis* obtained under nitrogen atmosphere.

by Dulong's formula. Fourier transform infrared (FT-IR) analysis of the raw material was also carried out using a Varian model Scimitar 2000 to identify structural groups using potassium bromide as transparent pellets. Table 1 gives the results of ultimate and proximate analyses of *E. spectabilis*. Fig. 1 shows the FT-IR spectra of raw material. The raw *E. spectabilis* was characterized by FT-IR in the middle region including the wave numbers between 4000 and 550 cm^{-1}. The aim of the analysis was to identify the functional groups of the raw material. According to literature [21–24], the bands in the spectra of raw *E. spectabilis* prove that it is mainly composed of lignin, cellulose and hemicelluloses. The band at 3328.70 cm^{-1} is formed by the hydroxyl group of lignin in *E. spectabilis*. The absorption at wave number of 1728.8 cm^{-1} is the characteristic of xylans of hemicellulose. The absorption peaks at about 2919.68 and 1316.93 cm^{-1} are the characteristics of cellulose. Generally the spectrum of lignin gives the similar absorption peaks. The absorptions at 2919.68, 1606.60 and 1007.57 cm^{-1} represent the lignin; especially the sharp peak at 1007.57 cm^{-1} is due to the ether bonds present in raw material.

Prior to exprerimental study, thermal behavior of the raw material was also investigated by thermogravimetric (TG) and differential thermal analysis (DTA). Thermal analysis was conducted with approximately 9.15 mg sample, operating at a heating rate of 10 °C/min from 25 °C to 850 °C with 10 mL/min nitrogen gas flow rate. The thermogravimetric weight loss and the corresponding derivative curves are given in Fig. 2. When TG curve is examined, approximately 7% weight loss until 110 °C shows the amount of moisture content of raw material which is close to the value given in Table 1. Hemicelluloses and cellulose of the raw material, the main components of biomass, start to decompose at 215.5 °C. The temperature at which the maximum decomposition occurs is approximately determined as 400 °C. All of the components (hemicelluloses, cellulose and lignin) of the raw material decompose very rapidly at this temperature reaching a maximum

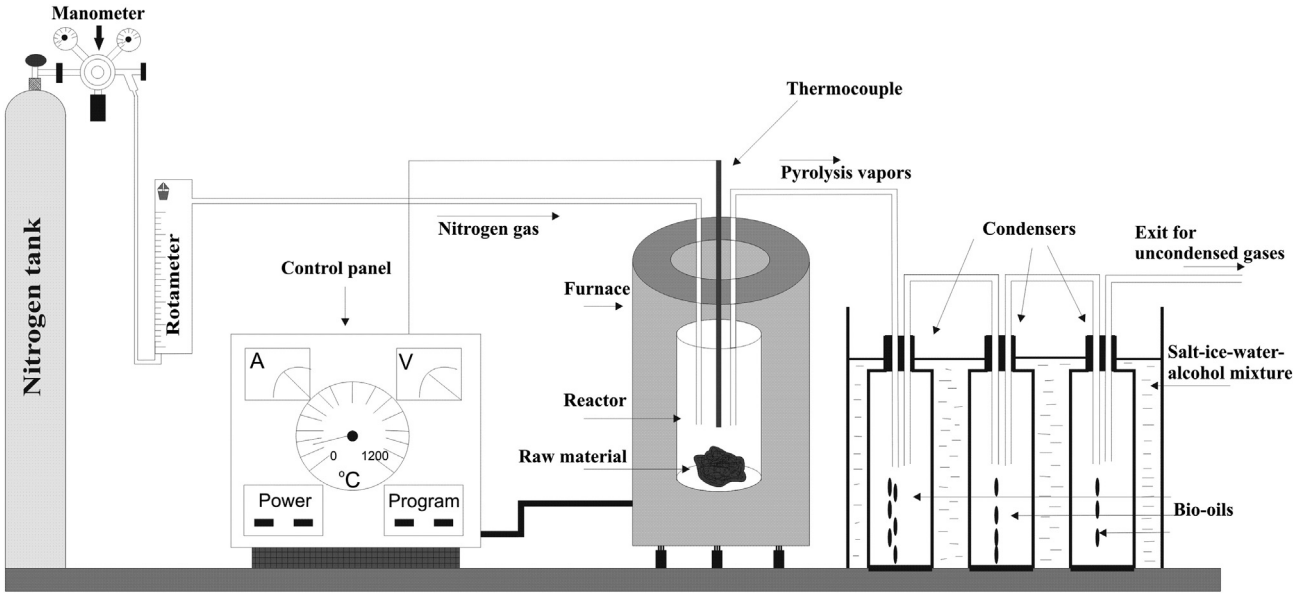

Fig. 3. Schematic diagram for the fixed-bed tubular reactor system.

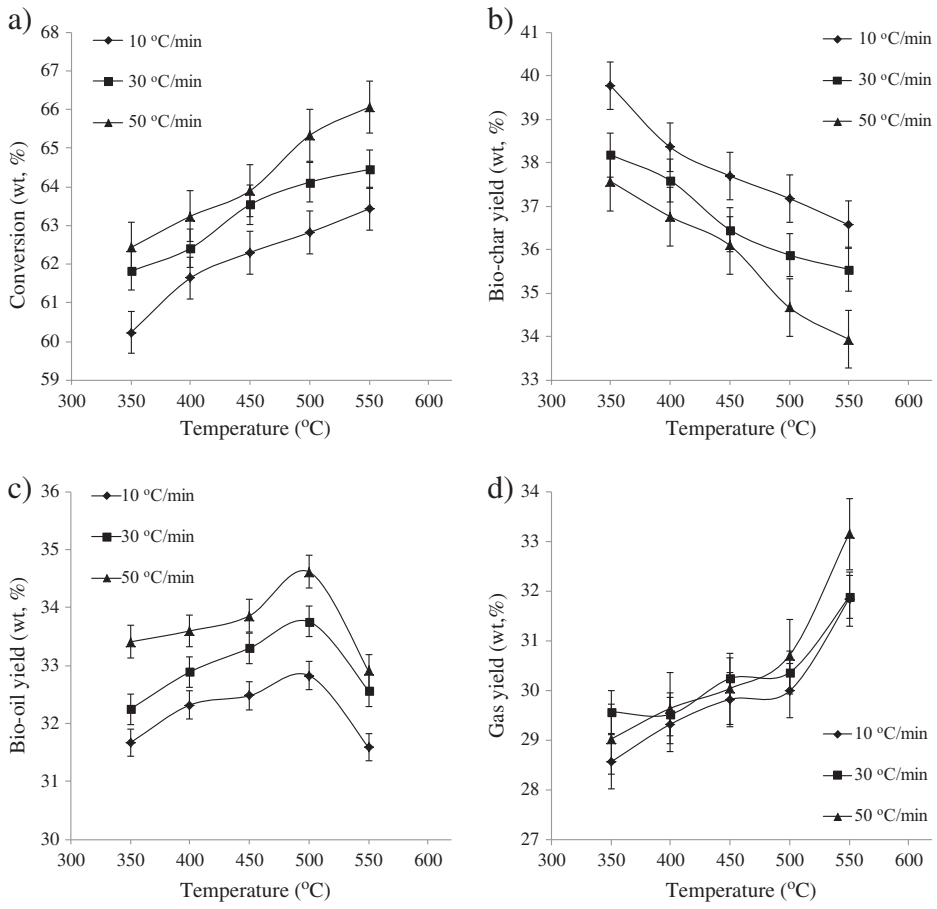

Fig. 4. The effect of temperature and heating rate on products yields (particle size: 0.224 > Dp > 0.150 mm, sweeping gas flow rate: 100 mL/min).

weight loss. The maximum weight loss (62.1%) of the raw material was occurred between 215.5 and 500 °C. After 500 °C, rate of decomposition gradually decreases and gets a minimum approximately at 650 °C. After 650 °C, the difference is that weight loss gets smaller and becomes almost zero at 800 °C [5,25]. The high amount of substances left behind (32%) after 800 °C is related to the content of fixed carbon and inorganic materials (ash) in raw material which are not decomposed at this temperature.

2.2. Experimental procedure

The pyrolysis experiments were performed in a fixed-bed tubular reactor made of stainless steel equipped with connection for inert gas input. Schematic diagram for the fixed-bed tubular reactor system is

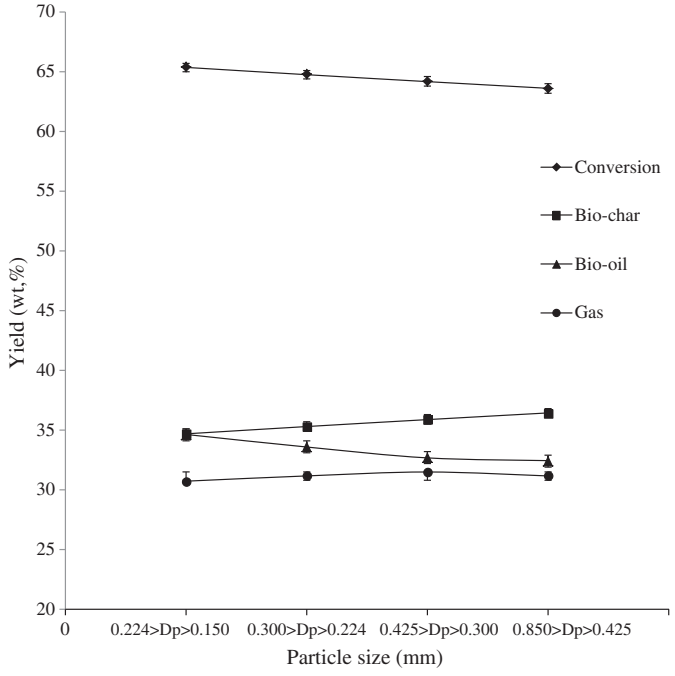

Fig. 5. The effect of particle size on product yields (temperature: 500 °C, heating rate: 50 °C/min, sweeping gas flow rate: 100 mL/min).

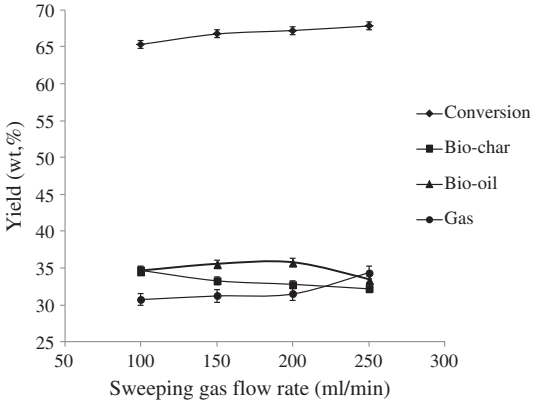

Fig. 6. The effect of sweeping gas flow rate on product yields (temperature: 500 °C, heating rate: 50 °C/min, particle size: 0.224 > Dp > 0.150 mm).

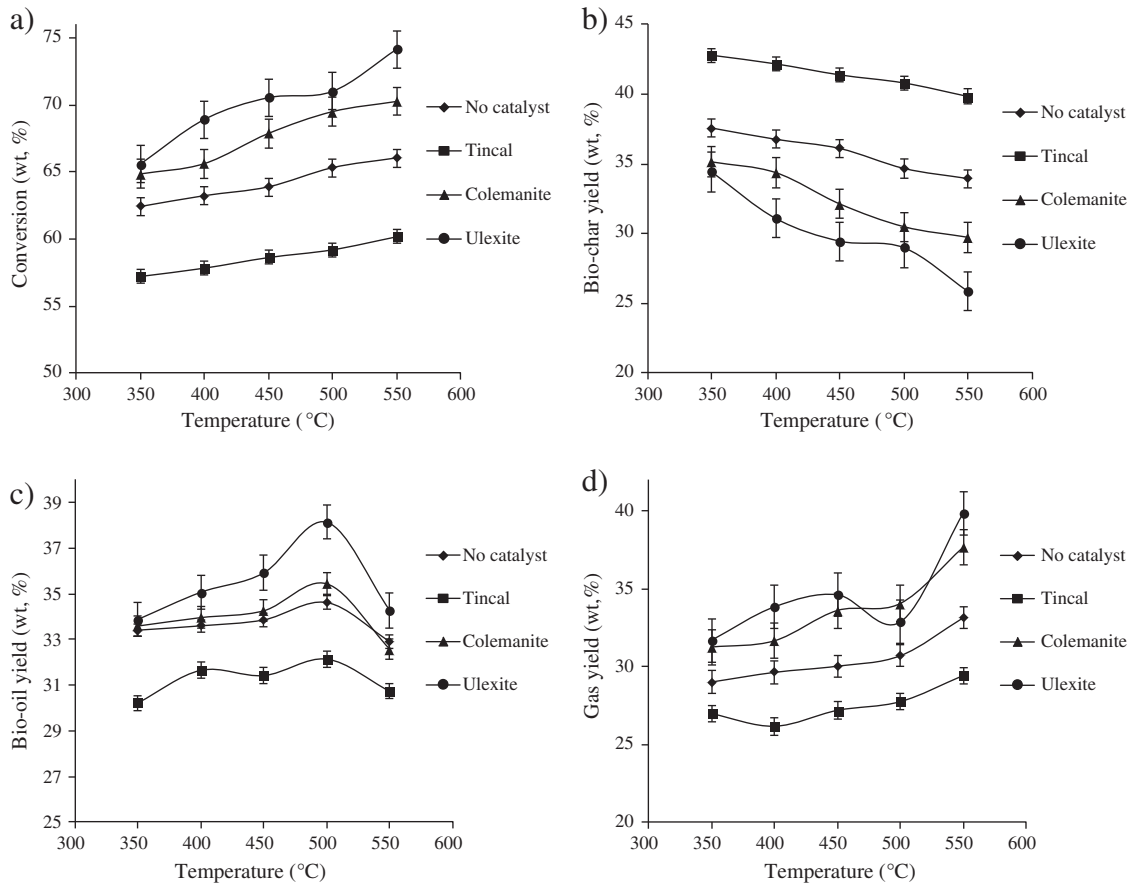

Fig. 7. The effect of catalysts on products yields (particle size: 0.224 > Dp > 0.150 mm, sweeping gas flow rate: 100 mL/min).

given in Fig. 3. In each trial, 20 g of raw material was put inside the reactor, closed tightly with connections for inert gas entry and products output pipe connected to liquid product collecting bottles. The reactor was heated externally by an electric furnace and the temperature is controlled by a NiCr–Ni thermocouple. The liquid collecting bottles were cooled to −10 °C using frozen salt-ethanol and water mixture

Table 2
The results of elemental analyses[a] of bio-chars obtained at 350, 450 and 550 °C.

Temperature	Without catalyst	With tincal	With colemanite	With ulexite
350 °C				
Carbon	61.75	60.49	62.82	64.51
Hydrogen	3.28	3.33	3.50	3.29
Nitrogen	0.87	0.81	0.77	0.91
Oxygen[b]	34.10	35.40	32.91	31.29
H/C molar ratio	0.63	0.66	0.67	0.61
O/C molar ratio	0.41	0.44	0.39	0.36
HHV (MJ/kg)	19.47	18.88	20.36	20.92
450 °C				
Carbon	66.24	65.24	64.93	66.93
Hydrogen	3.41	3.36	3.45	3.38
Nitrogen	0.73	0.78	0.70	0.86
Oxygen[b]	29.62	30.62	30.92	28.83
H/C molar ratio	0.61	0.62	0.63	0.60
O/C molar ratio	0.33	0.35	0.35	0.32
HHV (MJ/kg)	21.98	21.29	21.36	22.31
550 °C				
Carbon	69.17	67.25	68.04	67.64
Hydrogen	3.35	3.19	3.25	3.30
Nitrogen	0.81	0.74	0.72	0.73
Oxygen[b]	26.67	28.82	27.99	28.33
H/C molar ratio	0.58	0.57	0.57	0.59
O/C molar ratio	0.29	0.32	0.31	0.31
HHV (MJ/kg)	23.42	22.15	22.65	22.53

[a] Weight percentage on dry and ash free basis.
[b] By difference.

Table 3
The results of elemental analyses[a] of bio-oils obtained at 350, 450 and 550 °C.

Temperature	Without catalyst	With tincal	With colemanite	With ulexite
350 °C				
Carbon	54.38	52.26	55.84	55.64
Hydrogen	7.21	6.94	7.13	6.88
Nitrogen	1.35	1.31	1.35	1.44
Oxygen[b]	37.06	39.49	35.68	36.04
H/C molar ratio	1.59	1.59	1.53	1.48
O/C molar ratio	0.51	0.56	0.48	0.49
HHV (MJ/kg)	22.11	20.57	22.74	22.25
450 °C				
Carbon	55.78	54.38	57.56	57.47
Hydrogen	7.03	6.89	6.94	6.79
Nitrogen	1.41	1.27	1.36	1.40
Oxygen[b]	35.78	37.46	34.14	34.34
H/C molar ratio	1.51	1.52	1.45	1.42
O/C molar ratio	0.48	0.52	0.44	0.45
HHV (MJ/kg)	22.56	21.58	23.32	23.04
550 °C				
Carbon	58.96	57.73	58.34	59.71
Hydrogen	6.77	6.98	6.82	6.93
Nitrogen	1.46	1.22	1.34	1.37
Oxygen[b]	32.81	34.07	33.50	31.99
H/C molar ratio	1.38	1.45	1.40	1.39
O/C molar ratio	0.42	0.44	0.43	0.40
HHV (MJ/kg)	23.79	23.45	23.53	24.42

[a] Weight percentage on dry and ash free basis.
[b] By difference.

and the temperature was kept constant as −10 °C until no more gas is evolved. The gas product was discharged into a chimney through a hose and a fan. During the whole pyrolysis process, nitrogen gas is circulated to provide the inert atmosphere inside the reactor.

The pyrolysis experiments were performed in four series. In the first one, experiments without catalyst at five different temperatures ranging from 350 °C to 550 °C with heating rates of 10, 30, and 50 °C/min were carried out to investigate the effect of temperature and heating rate. The condensed liquid products which contain an aqueous (pyrolignic acid) and oil (pyrolytic oil) phase were collected in bottles. They were washed with dichloromethane, put in a separating funnel and separated from each other by decantation. Pyrolytic oil or bio-oil is dried with anhydrous sodium sulfate and recovered by evaporating the solvent in a rotary evaporator at temperature of 313 K and reduced pressure of 11 kPa and its yield (liquid) was calculated. After cooling, the amount of solid (bio-char) left behind was removed and weighed. The conversion of raw material to liquid and gaseous products was calculated by subtraction of amount of solid (bio-char) left behind in the reactor. The amount of gas evolved was calculated by subtraction of amount of solid and liquid products from 20, the amount of initial raw material. The following equations were used to calculate the conversion and product yields.

$$\text{Conversion}(\%) = \frac{\left(W_{\text{Biomass,db}} - W_{\text{Solid,db}}\right)}{W_{\text{biomass,db}}} \times 100 \quad (1)$$

$$\text{Liquid yield}(\text{wt.}\%) = \frac{\left(W_{\text{Liquid}}\right)}{W_{\text{Biomass,db}}} \times 100 \quad (2)$$

$$\text{Solid yield}(\text{wt.}\%) = \frac{\left(W_{\text{Solid,db}}\right)}{W_{\text{Biomass,db}}} \times 100 \quad (3)$$

$$\text{Gas yield}(\text{wt.}\%) = 100\%\text{–liquid yield}(\text{wt.}\%)\text{–solid yield}(\text{wt.}\%) \quad (4)$$

where $W_{\text{Biomass, db}}$ and $W_{\text{Solid, db}}$ are the weights of initial biomass and remaining solid (bio-char) respectively on dry basis.

From the first group of experiments, it was found that the optimum conditions for pyrolysis were 500 °C and 50 °C/min heating rate in the non-catalytic runs. In the second step, three boron minerals with constant ratio (10%) were added to reactor and pyrolysis experiments were performed at the same temperatures used in non-catalytic runs to investigate the effect of catalysts. After completion, the product yields were calculated and expressed on dry and ash free basis. The third group of experiments were performed with three more different particle size (0.850 > Dp > 0.425, 0.425 > Dp > 0.300, 0.300 > Dp > 0.224) samples to determine the effect of particle size. The last group was performed with four different sweeping gas flow rates of 100, 150, 200 and 250 mL/min to determine the effect of sweeping gas (N_2) flow rate on the product yields.

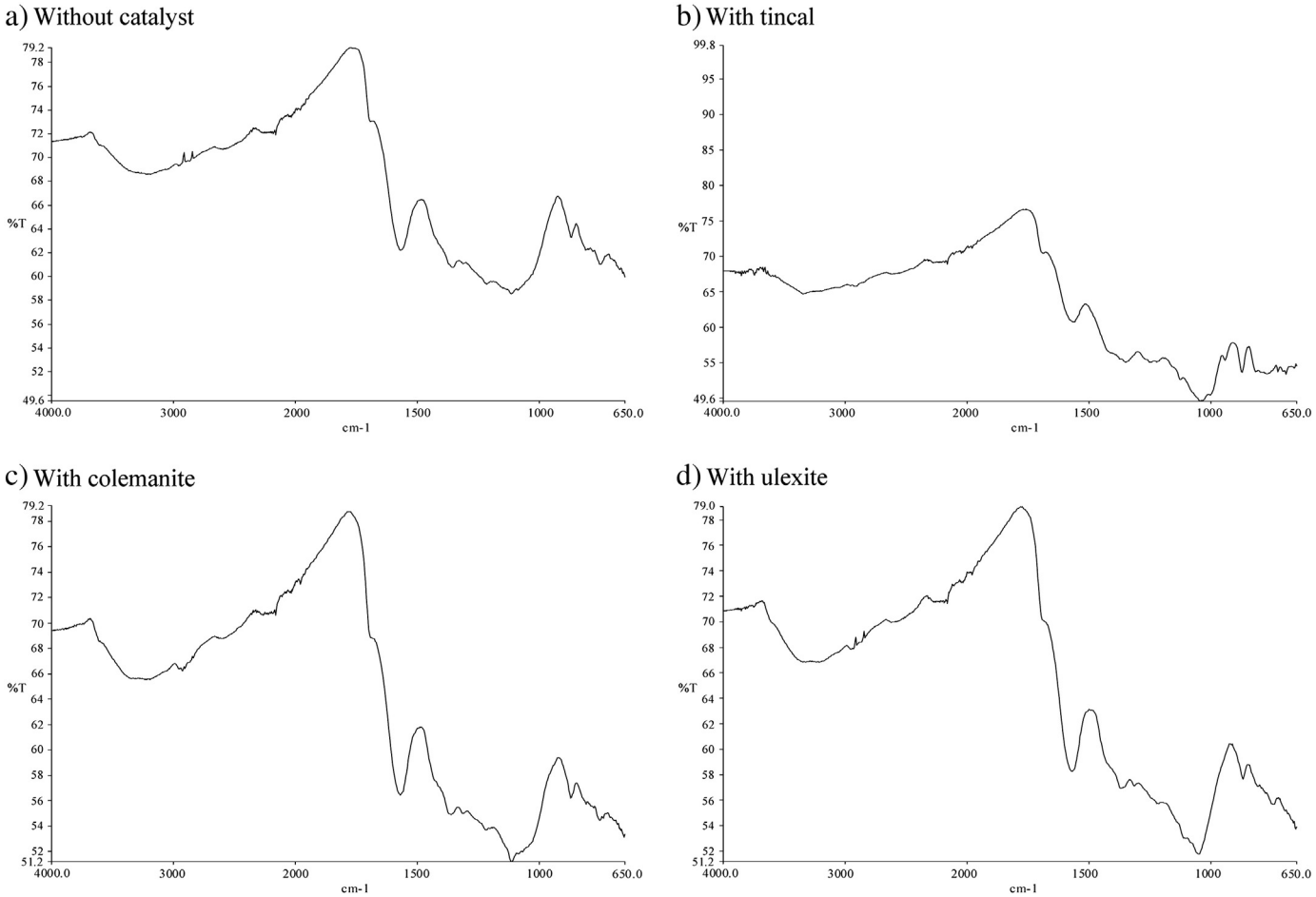

Fig. 8. FT-IR spectrums of bio-chars obtained at 350 °C.

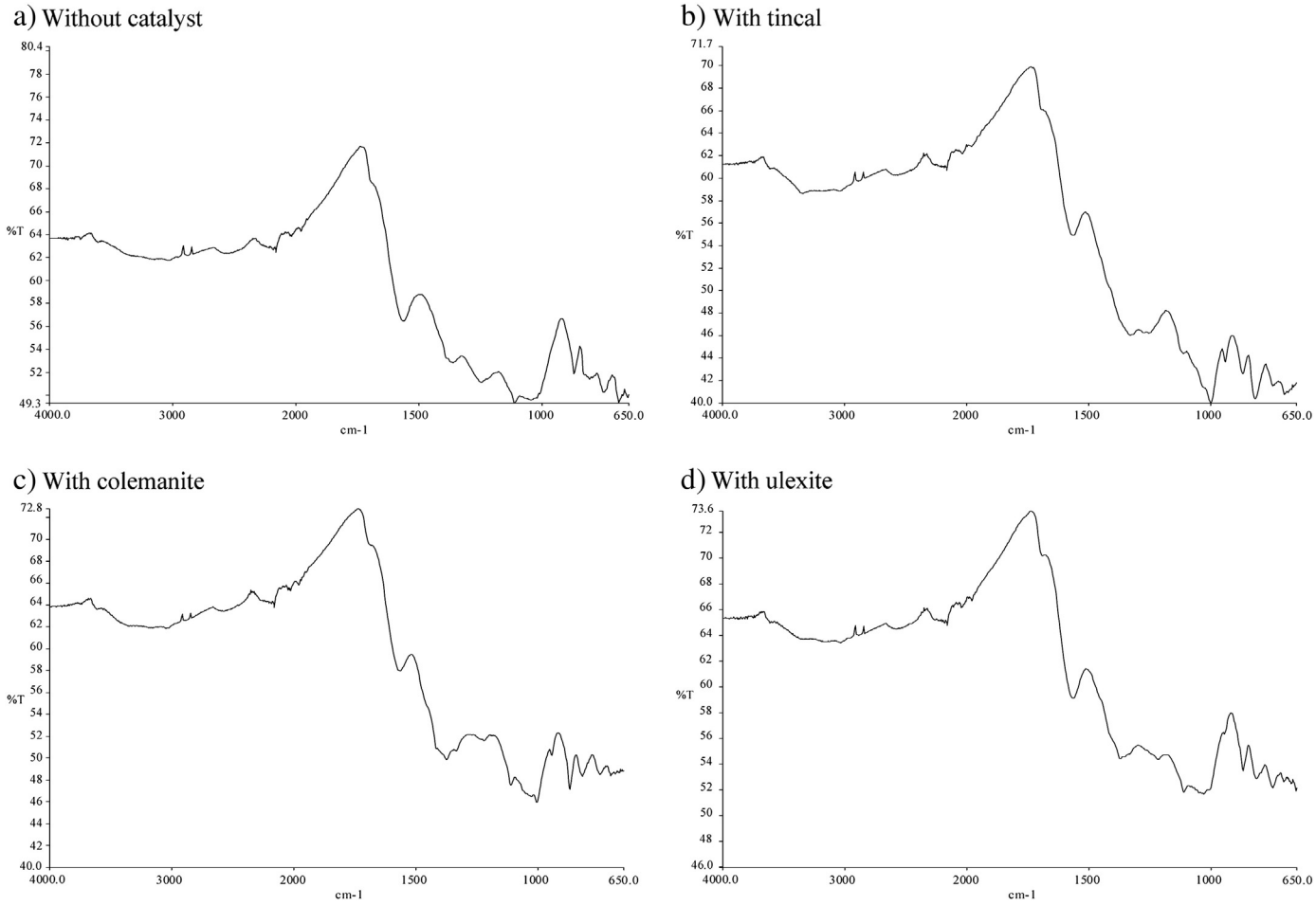

Fig. 9. FT-IR spectrums of bio-chars obtained at 550 °C.

2.3. Product analysis

The produced bio-chars and bio-oils at 350, 450 and 550 °C were analyzed and characterized by chromatographic and spectroscopic techniques using elemental, FT-IR and GC–MS analysis. Elemental analysis was performed with LECO CHNS 932 analyzer and infrared analysis with a PerkinElmer Spectrum 100 Spectrophotometer. The GC–MS analysis was performed on Agilent GC–MS 7890A/5975C series (Agilent Technologies, Santa Clara, CA). The column (HP-INNOWAX, length: 60 m, I.D.: 0.250 mm, film: 0.25 μm and temperature limits: from 40 °C to 260 °C) and injector temperatures were the same as those for GC. The carrier gas was helium at a flow rate of 1.7 mL/min. Samples of 1 μL were injected with a split ratio of 1:30. The GC oven temperature program was as follows: started at 40 °C; held for 10 min, raised from 40 °C to 200 °C with 5 °C/min heating rate; held for 15 min, raised to 240 °C with 10 °C/min heating rate; held for 15 min, raised to 260 °C with 10 °C/min heating rate; and held at this final temperature for 10 min. The column was directly introduced into the ion source of an Agilent 5975 series mass selective detector operating with an electron impact (EI) ionization mode. Chemical constituents were identified by comparison of their retention indices with literature values [26,27] and their mass spectral data with those from the W8N05ST.L, ADAMS.1 and Flavor3.L mass spectral databases.

3. Results and discussion

3.1. Effect of temperature and heating rate on product yields

The effect of temperature and heating rate on product yields is given in Fig. 4. It is seen from Fig. 4 that temperature had a positive effect on conversion at all heating rates. Bio-oil yields, on the other hand, were effected positively until 500 °C and increased until that temperature. After 500 °C, bio-oil yields decreased sharply at all heating rates. According to results, when temperature was increased from 350 to 500 °C, bio-oil yields were increased from 31.67% to 32.83% at a heating rate of 10 °C/min, from 32.25% to 33.76% at a heating rate of 30 °C/min and from 33.41% to 34.62% at a heating rate of 50 °C/min. Thus, the highest bio-oil yield was obtained at 500 °C at a heating rate of 50 °C/min in the non-catalytic runs. However, increases in yields were relatively smaller than expected between 350 to 500 °C, just 3.62% for 50 °C/min heating rate. After 500 °C, while the conversions were increased steadily, bio-oil yields were decreased to 31.59%, 32.57%, and 32.91% at 550 °C at heating of rates of 10, 30, and 50 °C/min respectively.

Among various parameters used in pyrolysis, temperature is considered as the most effective one on product yields [28–32]. Maguyon and Capareda [33] evaluated the effects of temperature on pressurized pyrolysis of Nannochloropsis oculata based on products yields and characteristics. They found that an increase in liquid product yield was observed with an increase in temperature from 400 to 500 °C. The maximum liquid yield of 35% was obtained at 500 °C. In a most recent study [34], thermal and catalytic pyrolysis of Karanja seed was carried out in a semi batch reactor at different temperatures in order to find out the optimum conditions. It was found that temperature had a positive affinity towards the yield of oil and non-condensable gas. The liquid yield increased up to 550 °C and then decreased with increase in temperature to 600 °C. Literature reported that pyrolysis at elevated temperature produce more amount of H_2 and CO which results in less liquid yield. The release of gases may be due to the reduction reaction of char at high temperatures.

The gaseous product yields have increased constantly with increasing pyrolysis temperature at all heating rates while the amounts of solid were found to be decresing with increase in temperature. As seen in Fig. 4, when temperature is increased from 350 to 550 °C, the gaseous product yields were increased from 28.56% to 31.84% at a heating rate of 10 °C/min, from 29.57% to 31.88% at a heating rate of 30 °C/min and from 29.02% to 33.15% at a heating rate of 50 °C/min. As explained before, these results are because of the formation of secondary cracking reactions of the pyrolysis vapors. Furthermore, secondary decomposition of the bio-chars may result in the production of non-condensable gaseous substances at higher temperatures contributing an increase in gaseous products [5,35]. As for the effect of heating rate, there have been very slight changes in liquid product yields in the slow pyrolysis of biomass species when compared with fast pyrolysis. This result is in accordance to the reports in the literature [36,37]. The higher heating rate causes the solid material to a fast depolymerization to primary volatiles while the lower heating rate leads to a very slow and limited dehydration to more stable anhydrocellulose [38,39]. Solid product (bio-char) yields were decreased continuously with increasing the pyrolysis temperature at all heating rates because of greater primary decomposition of the biomass or secondary decomposition of the char residue, leading the higher conversions with increasing temperature. As pyrolysis temperature was increased from 350 to 550 °C, bio-char yields were decreased from 39.77% to 36.57% at a heating rate of 10 °C/min, from 38.18% to 35.55% at a heating rate of 30 °C/min and from 37.57% to 33.94% at a heating rate of 50 °C/min.

3.2. Effect of particle size on product yields

Particle size is known to influence pyrolysis and liquefaction yields. The effect of particle size (Dp) on product yields obtained in pyrolysis experiments at constant temperature of 500 °C and at a constant heating rate of 50 °C/min is given in Fig. 5. As seen in Fig. 5, change in particle size had no significant effect on product yields. The highest conversion and liquid yield were 65.33% and 34.62% obtained with a particle size of 0.224 > Dp > 0.150 mm respectively. When particle size was increased 0.224 > Dp > 0.150 to 0.850 > Dp > 0.425, gas and bio-char yields were increased from 30.71% to 31.15% and from 34.67% to 36.42% respectively while liquid yields were decreased from 34.62% to 32.43%. This is because of insufficient heat and mass transfer due to the large diameter of the particles, which in turn, caused lower reaction rates.

These results are consistent with the previous studies reported in literature [40,41]. An increase in particle size leads to greater temperature gradients inside the particles. The core temperature of the particles would be lower than the surface causing the higher bio-char and lower bio-oi yields. The effect of particle size can be explained in terms of heating rate and mass transfer limitation. The heat flux and the heating rate are higher in small particles than in large particles. The larger particles will heat up more slowly than small ones resulting in the lower temperature of average particles. This will cause the formation of less amounts of volatile yields. Uniform heating can be established with sufficiently small particle size samples. The higher heating rate favors a decrease of the solid

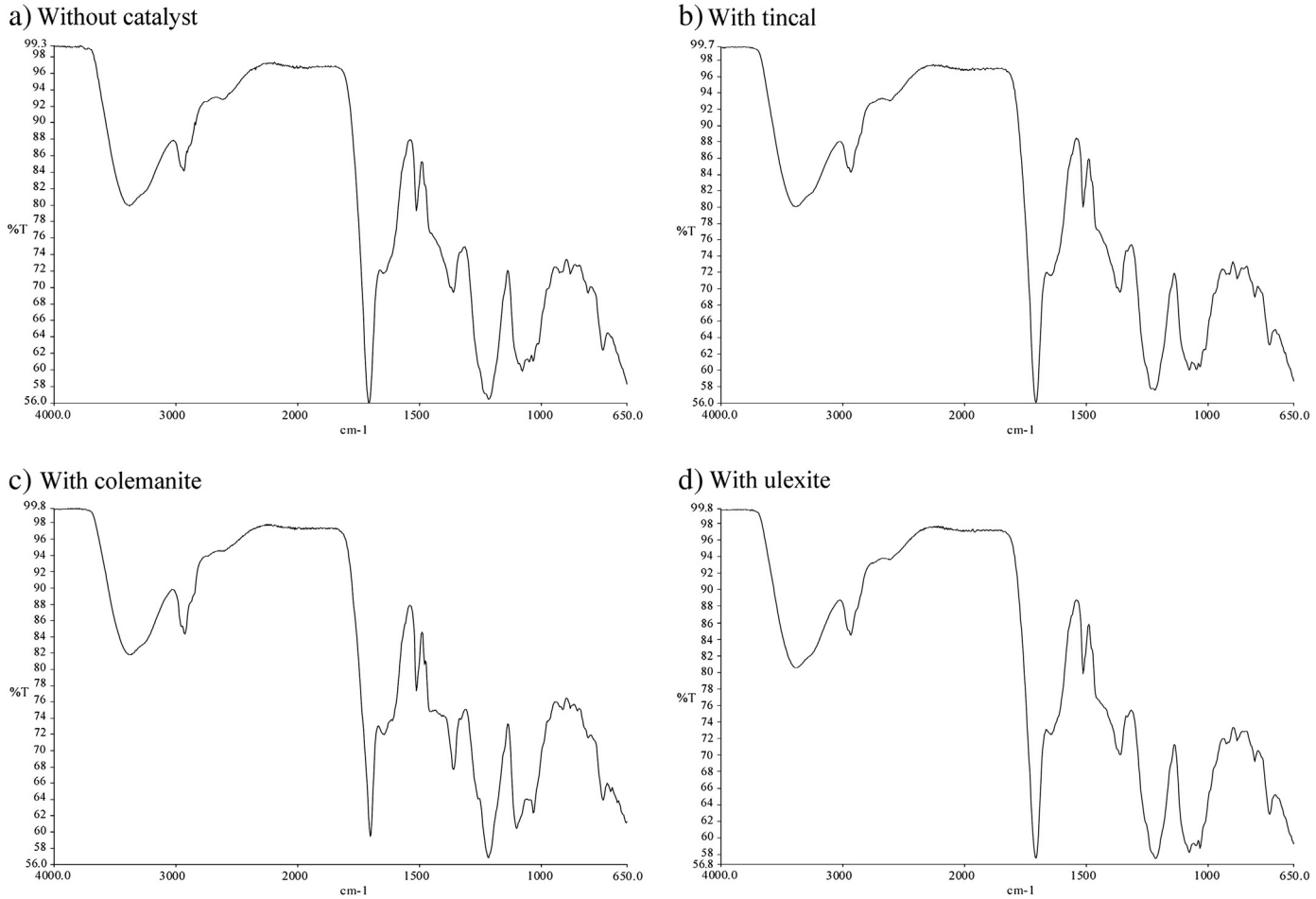

Fig. 10. FT-IR spectrums of bio-oils obtained at 350 °C.

yield. It has been reported that particle size less than 5 mm has no significant effect on the process rate in slow pyrolysis. The results of this study show that 0.224 > Dp > 0.150 mm particle size is the most suitable among all for obtaining high amounts of liquid from pyrolysis of *E. spectabilis* [5,42,43].

Shen et al. [44] have found a dramatic decrease in the yield of pyrolytic lignin when particle size of biomass was increased. In a recent work [45], the effect of particle size on the yield and composition of pyrolytic lignin was studied in a fluidized bed reactor. As the pyrolytic lignin yield was decreased, the char yield was increased. The maximum yield of 12% pyrolytic lignin was obtained with 0.30 mm wood particles and decreased drastically when the particle size is increased up to 3 mm.

3.3. Effect of sweeping gas flow rate on product yields

The effect of sweeping gas (N_2) flow rate on product yields was determined by performing the pyrolysis experiments with different nitrogen gas flow rates using the optimum conditions (particle size: 0.224 > Dp > 0.150, temperature: 500 °C, heating rate: 50 °C/min) obtained in the first group of experiments. Fig. 6 shows the effect of sweeping gas flow rate on product yields. From Fig. 6, the maximum liquid yield of 35.75% was obtained at a sweeping gas flow rate of 200 mL/min. The conversions and gas yields were increased with increasing sweeping gas flow rate while bio-char yields were decreased. The liquid yields were increased with increasing sweeping gas flow rate, reaching the maximum value at 200 mL/min, and then decreased at 250 mL/min. The function of sweeping gas is to remove the hot and the produced compounds from the hot zone as quickly as possible and reduce the residence time of hot vapors. The minimization of secondary reactions such as thermal cracking, repolymerisation and recondensation can be achieved with higher velocity of the sweeping gas that transfers the hot vapors into the condensation vessels. At lower sweeping gas flow rates, the velocity of the gas was not enough to transfer the hot vapors into the condensation section. Increasing the flow rate to 200 mL/min has maximized the bio-oil yield. However, changes in products yields occured with small increments. The liquid yields were increased from 34.62% to 35.75%, when nitrogen flow rate was increased from 100 mL/min to 200 mL/min and then decreased to 33.46% at 250 mL/min flow rate. This reduction may be due to the insufficient cooling by condensation apparatus in the system and fast leaving of the hot pyrolysis vapors before condensation. The gas yields were increased from 30.71% to 34.37%, when nitrogen flow rate was increased from 100 mL/min to 250 mL/min. As for bio-char yield, it decreased to its minimum value of 32.17% as nitrogen flow rate was increased from 100 mL/min to 250 mL/min. These results are in accordance with previous studies reported in literature [46–48].

In a previous study [49], pyrolysis of empty fruit bunch was conducted using a fixed-bed reactor to determine the effects of holding time and the sweeping nitrogen gas flow rates on product yields. It was found that the maximum bio-oil yield of 46.02% was obtained at nitrogen flow rate of 200 mL/min. In a recent study [50], sweeping gas influence on the empty fruit bunch pyrolysis product yields was investigated by varying the N_2 flow rates. The maximum bio-oil percentage yield from the $Ca(OH)_2$ catalyzed pyrolysis was obtained at sweeping gas flow rate of 200 mL/min.

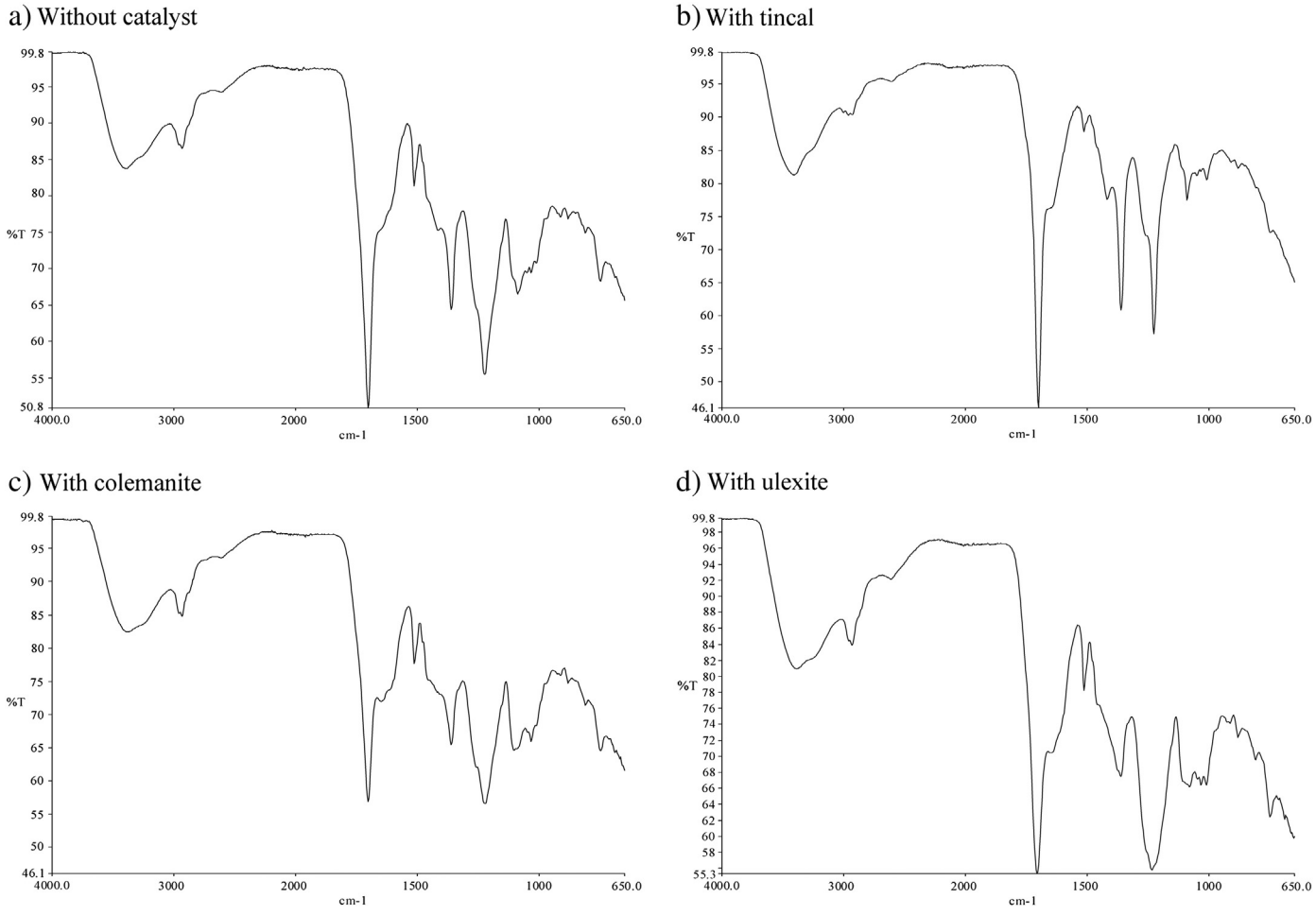

Fig. 11. FT-IR spectrums of bio-oils obtained at 550 °C.

Table 4
Main chemical compounds present in bio-oils obtained at 350 °C.

No.	Compound types	Relative abundance (% area)			
		Without catalyst	With tincal	With colemanite	With ulexite
1	Ethanone, 1-(2-furanyl)-	1.82	–	–	1.20
2	2,4-Hexadiene, 2,5-dimethyl-	–	1.11	0.60	–
3	1,2-Cyclopentanedione	–	0.74	–	1.31
4	3-Hexanone	–	0.37	–	0.35
5	2-Butanone, 1-(acetyloxy)-	–	0.31	–	0.33
6	Piperidine, 1-methyl-	0.64	–	–	–
7	Phenol	5.37	3.80	3.59	3.98
8	2(5H)-Furanone	2.27	2.43	1.20	2.31
9	Furfuryl acetate	–	–	–	0.26
10	Furfural<5-methyl->	0.85	1.15	–	1.09
11	2-Cyclopenten-1-one, 3-methyl-	1.35	1.12	0.90	1.16
12	Octanoic acid, 2-tetrahydrofurylmethyl ester	–	–	0.89	–
13	Cyclopentanone, 2,5-dimethyl-	–	–	0.49	–
14	Butanoic acid, propyl ester	4.07	2.85	–	3.81
15	2(5H)-furanone, 3-methyl-	0.53	0.52	–	0.52
16	Cyclohexanone, 3-methyl-, (R)-	–	–	–	0.91
17	Acetaldehyde, methyl(2-propenyl)hydrazone	0.70	0.84	–	–
18	2-Cyclopenten-1-one, 2-hydroxy-3-methyl-	8.07	7.83	6.98	7.15
19	3,4-Dimethyl-1,2-cyclopentadione	0.50	0.47	1.04	0.47
20	2-Cyclopenten-1-one, 2,3-dimethyl-	0.81	0.69	0.73	0.71
21	p-Cresol	1.73	1.47	1.28	1.37
22	m-Cresol	1.27	1.20	0.98	1.06
23	Triallylphosphine	–	–	0.41	–
24	Carbonic acid, isobutyl isohexyl ester	–	0.52	–	–
25	2-Vinyl-9-[3-deoxy-β-d-ribofuranosyl]hypoxanthine	0.47	–	–	–
26	Lactic acid, 2-methyl-, monoanhydride with 1-butaneboronic acid, cyclic ester	–	–	–	0.41
27	Guaiacol	14.69	11.85	12.87	12.87
28	Cyclohexane, (1-methylethylidene)-	–	–	–	0.50
29	2-Cyclopenten-1-one, 2,3,4-trimethyl-	–	–	0.52	–
30	3-Ethylcyclopent-2-en-1-one	–	–	0.43	–
31	4-Octene, 2-methyl-, (z)-	–	–	0.71	–
32	Phenol, 2-ethyl-	–	–	0.45	–
33	3,5-Dimethylcyclopentene	–	0.60	–	–
34	6-Methyl-1,5-heptadiene	–	0.47	–	–
35	1,3-Pentadiene, 2,3-dimethyl-	0.54	–	–	–
36	1-Cyclohexene-1-carboxaldehyde	0.52	–	–	–
37	2-Cyclopenten-1-one, 3-ethyl-2-hydroxy-	3.23	3.36	2.58	4.11
38	Cyclohexane, 1,1-dimethyl-	–	–	–	0.53
39	2-Methoxybenzenethiol	–	–	0.60	–
40	6-Oxo-1,6-dihydro-pyridazine-3-carboxylic acid	–	–	1.08	–
41	Oxireno[4,5]cyclopenta[1,2-c]pyran-2(1AH)-one, hexahydro-5a,6-dihydroxy-1a-methyl-, (1aα,1bβ,5aβ,6α,6aα)-	–	–	–	0.42
42	2-Furancarboxaldehyde, 5-(hydroxymethyl)-	–	0.52	–	–
43	3-Cyclohexen-1-carboxaldehyde, 3-methyl-	–	0.39	–	–
44	4-Hexen-3-one, 4,5-dimethyl-	0.60	–	–	–
45	Phenol, 2,4-dimethyl-	–	0.29	–	–
46	Octane, 2,6-dimethyl-	2.39	1.90	1.95	2.06
47	2-Methoxy-3-methylphenol	–	–	–	0.31
48	2-Methoxy-6-methylphenol	–	–	0.38	–
49	Phenol, 2-methoxy-3-methyl-	–	0.34	–	–
50	Phenol, 2-methoxy-4-methyl-	0.48	–	–	–
51	1,2-Benzenediol	2.22	1.66	0.88	1.88
52	1-Hydroxy-2-methoxy-4-methylbenzene	–	–	–	0.84
53	Benzene, 1,4-dimethoxy-	–	0.85	0.75	–
54	Cresol<2-methoxy-para->	3.66	4.47	3.58	4.13
55	2-Hydroxy-3-propyl-2-cyclopenten-1-one	–	–	–	0.45
56	Toluene, 3,4-dimethoxy-	–	–	–	0.50
57	2-Cyclopenten-1-one, 2-hydroxy-3-propyl-	–	–	0.61	–
58	2-Methyl-3-isopropylpyrazine	–	–	0.52	–
59	2,3-Dimethoxytoluene	–	–	0.68	–
60	2(3H)-Furanone, 5-ethyldihydro-	–	–	2.17	2.72
61	1-(3-Methoxy-2-pyrazinyl) ethanone	–	0.58	–	–
62	4-Octanone, 5-hydroxy-2,7-dimethyl-	–	3.64	–	–
63	Benzeneethanol, 2-methoxy-	–	4.47	4.74	4.56
64	Benzene, 1,2-dimethoxy-4-methyl-	0.58	–	–	–
65	4-Ethylbutan-4-olide	2.46	–	–	–
66	Guaiacol, 4-ethyl-	4.24	–	–	–
67	1,2-Benzenediol, 3-methoxy-	2.11	2.47	1.85	2.59
68	1(2H)-Pentalenone, hexahydro-5,5-dimethyl-, cis-(±)-	–	–	0.47	–
69	Hydroquinone	0.60	0.87	0.72	0.84
70	2-Methoxy-4-vinylphenol	2.50	1.71	3.08	1.40
71	1H-Inden-1-one, 2,3-dihydro-	0.47	0.45	0.47	0.43
72	Phenol, 2-methoxy-4-propyl-	–	–	1.61	–

(continued on next page)

Table 4 *(continued)*

No.	Compound types	Relative abundance (% area)			
		Without catalyst	With tincal	With colemanite	With ulexite
73	2-(1,2-Epoxycyclohexyl)-1-pentene	1.41	–	–	1.40
74	2,6-Dimethoxyphenol	14.44	14.99	20.51	15.28
75	Isoeugenol	0.46	0.38	0.43	0.41
76	Benzaldehyde, 3-hydroxy-4-methoxy-	–	–	–	0.48
77	Eugenol	2.34	2.33	2.74	2.19
78	Benzoic acid, 4-hydroxy-3-methoxy-	2.07	2.85	2.79	2.52
79	3-Furancarboxylic acid, 5-ethyl-2, 4-dimethyl-, methyl ester	2.77	3.11	3.84	3.20
80	Ethenamine, 2-(1-cyclopenten-1-yl)-n,n-dimethyl-, (e)-	–	–	–	1.13
81	2-Methoxy-4-propyl-phenol	1.08	1.35	0.98	–
82	Homovanillyl alcohol	–	1.11	–	–
83	4,11-Dioxa-3,5-dimethyltetracycloundecane cage compound	–	0.84	1.55	0.70
84	Benzaldehyde, 4-[[4-(acetyloxy)-3,5-dimethoxyphenyl]methoxy]-3-methoxy-	–	–	–	0.38
85	1,4-Dihydrophenanthrene	0.96	–	–	–
86	1-(2,5-Dimethoxyphenyl)-propanol	–	0.39	0.50	
87	Phenol, 2,6-dimethoxy-4-(2-propenyl)-	1.59	2.19	2.32	1.99
88	1-Butanone, 1-(2,4,6-trihydroxy-3- methylphenyl)-	0.65	–	–	–
89	1-(1-Hydroxybutyl)-2,5-dimethoxybenzene	–	–	0.59	–
90	Thiophene, 2-isobutyl-5-isopentyl-	–	0.67	–	0.79

3.4. Effects of catalysts on product yields

The effects of catalysts on conversion are given in Fig. 7. Experiments with catalysts were performed at a constant heating rate of 50 °C/min using 0.224 > Dp > 0.150 mm particle size sample and 100 mL/min sweeping gas flow rate at the same temperatures used in non-catalytic runs to determine the effects of catalysts on the product yields. As seen from Fig. 7, catalysts had different effects on product yields. Colemanite and ulexite have increased the conversions with increasing temperature compared with non-catalytic runs. Among them, ulexite was more effective than colemanite in terms of conversion. The addition of tincal, on the other hand, decreased the conversions at all pyrolysis temperatures. The highest conversion of 74.15% was obtained with 10% ulexite in the catalytic runs at 550 °C. As for the liquid yields, effects of catalysts were different from each other. Liquid yield obtained with colemanite and ulexite was higher than non-catalytic runs at all. Tincal has again decreased the liquid yields at all temperatures. Without exceptions, experiments performed with all catalysts, liquid (bio-oil) yields have increased steadily with increasing temperature until 500 °C and then decreased at 550 °C (Fig. 7). The liquid yield, which was 34.62% without catalyst, reached the maximum value of 38.14% with 10% ulexite at 500 °C. The gas yields were increased with temperature while bio-char yields were decreased steadily in both catalytic and non-catalytic runs at almost all temperatures except with ulexite at 500 °C. The gas yields with ulexite at 500 °C did not follow the tendency of increasing with temperature. There was a decrease in gas yield at 500 °C with ulexite. This may be due to the formation of highest amount of liquid products at 500 °C with ulexite. The gas yields were increased from 31.27% to 37.69% when temperature was increased from 350 to 550 °C in the catalytic run with colemanite. Similar results were obtained with tincal.

The liquid product obtained in pyrolysis contains an aqueous phase and bio-oil or oil phase which is generally called as pyrolytic liquid. It is a black liquid containing highly oxygenated compounds used as boiler fuel in power stations for heat production. If it is intended to be used as transportation fuels, they should be upgraded first by hydrodeoxygenation to produce aromatics or hydrocarbons, or catalytic cracking by using zeolite to produce light aromatic hydrocarbons and light alkanes. There are numerous reports of pyrolysis and liquefaction regarding the effect of catalysts on product yields in literature [51–55]. The usage of catalyst can make significant changes on product yiels and properties of bio-oils. In general, addition of catalyst had positive effect and increased the bio-oil yields while in some studies, it had negative effect and decreased the bio-oil yields. Furthermore, the addition of catalyst has changed the composition of bio-oils. Naqvi et al. [56] conducted catalytic (zeolite ZSM-5) pyrolysis of paddy husk in a drop type pyrolyzer for bio-oil production and investigated the role of temperature and catalyst on product yields and composition. The presence of catalyst culminated in less bio-oil yield coupled with higher calorific values and high water contents in comparison to non-catalytic pyrolysis. Shao et al. [57] investigated the catalytic effect of metal oxides on pyrolysis of sewage sludge. They found that the presence of ZnO and Fe_2O_3 probably inhibited the decomposition of organic matters in demineralized sludge samples to generate more solid residues, while Al_2O_3, CaO, and TiO_2 promoted the degradation of organic matters throughout the whole pyrolysis temperature ranges. In another study, catalytic effects of NaOH and Na_2CO_3 additives on alkali lignin pyrolysis and gasification were examined. The results showed that the reaction can be catalyzed by NaOH and Na_2CO_3 but analysis proved that the influences of additives on products mainly varied in amounts, not in species [58]. In a recent study, hydrothermal liquefaction of beech wood was carried out using borax decahydrate and sodium borohydride as catalyst. It was found that the use of both catalysts has increased bio-crude yields at all liquefaction temperatures [59].

3.5. Characterization of bio-chars and bio-oils by elemental, FT-IR and GC–MS analysis

The results of elemental analyses of bio-chars and bio-oils obtained at 350, 450 and 550 °C are given in Tables 2 and 3 respectively. Compared to carbon and oxygen contents of the raw material, all of the products (bio-chars and bio-oils) from pyrolysis have higher carbon and lower oxygen contents in both non-catalytic and catalytic runs, and accordingly have higher calorific values. As seen in Tables 2 and 3, the calorific values of bio-chars and bio-oils were higher than 18.18 MJ/kg and 20.57 MJ/kg respectively, in comparison with the low calorific value (13.17 MJ/kg) of the raw material.

FT-IR spectrums of bio-chars obtained at 350 and 550 °C are given in Figs. 8 and 9 respectively. Compared with raw material, there have been significant changes in the FT-IR spectrum as a result of pyrolysis. The O – H stretching vibration band at 3328 cm^{-1} has been almost dissappeared for bio-chars obtained at 350 °C and completely dissappeared for bio-chars obtained at 550 °C. This indicates that decomposition of raw material is not complete at 350 °C and continues with more heating. During the pyrolysis process, oxygen was removed from raw material causing the phenolic and aromatic structures to

Table 5
Main chemical compounds present in bio-oils obtained at 550 °C.

No.	Compound types	Relative abundance (% area)			
		Without catalyst	With tincal	With colemanite	With ulexite
1	1-(3H-Imidazol-4-yl)-ethanone	1.14	–	–	–
2	Cyclobutene, 1,3,3,4-tetramethyl-	–	–	–	1.49
3	Propane, 1,1′-oxybis[2-methyl-	0.28	–	–	–
4	2,4-Hexadiene, 2,5-dimethyl-	–	2.58	0.98	–
5	2-Butanone, 1-(acetyloxy)-	0.23	–	–	–
6	Phenol	4.70	9.75	5.70	6.75
7	2(5H)-Furanone	1.26	1.61	1.23	1.48
8	Furfuryl acetate	0.19	–	–	–
9	Furfural<5-methyl->	0.97	1.72	–	0.84
10	2-Cyclopenten-1-one, 3-methyl-	0.94	2.21	1.38	1.53
11	3-Buten-2-ol, 2-methyl-	–	–	1.06	–
12	Butyric acid hydrazide	–	2.45	–	–
13	Tetrahydro-2-furanylmethyl butyrate	2.13	–	–	–
14	1-Penten-3-ol, 2-methyl-	–	–	–	1.94
15	2(5H)-Furanone, 3-methyl-	0.31	–	–	0.33
16	Cyclohexanone, 3-methyl-, (R)-	–	–	–	0.53
17	1-Pyrroline, 3-ethyl-	0.51	–	–	
18	2-Nonadecanone, O-methyloxime	–	–	–	0.27
19	2-Cyclopenten-1-one, 2-hydroxy-3-methyl-	7.05	–	–	–
20	2-Cyclopenten-1-one, 3,5,5-trimethyl-	0.42	–	–	–
21	3,4-Dimethyl-1,2-cyclopentadione	0.39	–	0.95	0.46
22	2-Cyclopenten-1-one, 2,3-dimethyl-	0.71	1.57	1.17	1.07
23	o-Cresol	–	11.56	9.44	8.59
24	p-Cresol	2.03	4.21	2.70	2.79
25	m-Cresol	2.48	5.75	3.46	4.17
26	Oxalic acid, 6-ethyloct-3-yl heptyl ester	0.35	–	–	–
27	Guaiacol	9.45	10.18	12.29	10.80
28	Cyclohexene, 3-(1-methylethyl)-	–	–	–	0.60
29	1-Cyclohexene-1-carboxaldehyde	–	–	–	0.53
30	Ethanone, 1-(1-cyclohexen-1-yl)-	–	–	0.67	–
31	Cyclohexene, 1-ethyl-	–	–	0.50	–
32	Cyclohexane, (1-methylethylidene)-	0.52	–	–	–
33	2-Propanone, 1-(N-cyanomethylimino-)	0.36	–	–	–
34	2-Cyclopenten-1-one, 3-ethyl-2-hydroxy-	2.27	1.93	–	2.18
35	Phenol, 2,5-dimethyl-	–	1.67	–	1.01
36	Phenol, 2,3-dimethyl-	–	–	–	0.42
37	Phenol, 3,5-dimethyl-	–	1.61	–	–
38	Phenol, 2,6-dimethyl-	0.99	–	6.70	1.20
39	Phenol, 4-ethyl-	–	1.64	1.24	1.07
40	1,1-(Dimethyl)spiro[2.4]hepta-4-ene	–	–	–	1.46
41	Phenol, 3-ethyl-	–	1.48	1.46	
42	Phenol, 2-ethyl-	0.54	–	0.80	0.68
43	1-Methyl-2,3-cyclohexadione	–	–	2.09	–
44	Cyclohexane, 1,4-dimethoxy-2-methyl-, stereoisomer	0.28	–	–	–
45	Phenol, 2,4-dimethyl-	–	1.01	–	1.15
46	2-Butene, 1-methoxy-, (E)-	0.48	–	–	
47	Dimethyl phenol<2,6->	2.63	1.37	–	0.85
48	1-Hepten-3-ol-6,6-d2	2.28	–	–	–
49	2-Methoxy-3-methylphenol	0.25	–	–	0.36
50	Phenol, 2-methoxy-4-methyl-	0.61	–	–	–
51	1,2-Benzenediol	1.85	1.35	–	1.02
52	1-Hydroxy-2-methoxy-4-methylbenzene	3.84	–	–	0.69
53	2-Hydroxy-3-propyl-2-cyclopenten-1-one	0.39	–	–	–
54	Pyridine, 2-ethyl-6-methyl-	0.25	–	–	–
55	Benzene, 1-ethyl-4-methoxy-	0.21	–	0.87	–
56	Phenol, 4-methoxy-	0.21	–	–	–
57	2,4-Dimethoxytoluene	0.61	–	–	–
58	2(3H)-Furanone, 5-ethyldihydro-	2.36	–	1.92	2.01
59	Cresol<2-methoxy-para->	–	4.83	0.60	4.26
60	3-Methyl-4-ethylphenol	–	–	–	0.37
61	2,4-Pentadien-1-ol, 3-methyl-, (e)-	–	3.53	–	–
62	2-(2-Methyl-propenyl)-cyclohexanone	–	–	–	0.39
63	Benzeneethanol, 2-methoxy-	4.24	–	5.13	4.49
64	Guaiacol, 4-ethyl-	–	4.28	–	–
65	1,2-Benzenediol, 3-methoxy-	3.15	–	0.82	1.68
66	Hydroquinone	1.23	1.39	–	–
67	1-Methoxy-4-(1′-methylethyl)cyclohexa-1,4-diene	0.38	–	–	–
68	2-Hydroxy-3-propylpyrazin	–	–	–	0.75
69	Naphthalene, 2-methyl-	0.43	–	–	0.52
70	2-Methoxy-4-vinylphenol	3.55	3.40	3.04	2.51
71	1H-Inden-1-one, 2,3-dihydro-	0.52	0.89	0.72	0.74
72	2-Methoxy-4-propyl-phenol	–	–	1.59	–
73	Guaiacol, 4-propyl-	1.27	–	–	–

(continued on next page)

Table 5 *(continued)*

No.	Compound types	Relative abundance (% area)			
		Without catalyst	With tincal	With colemanite	With ulexite
74	1,3-Benzenediol, 2-methyl-	0.47	–	–	–
75	2-(1,2-Epoxycyclohexyl)-1-pentene	–	–	–	1.28
76	2,6-Dimethoxyphenol	11.14	9.76	16.30	11.48
77	2-Exo-(1-oxacyclohex-2-yloxy)bicyclo[2.2.1]hepta-5-ene	0.28	–	–	–
78	Isoeugenol	0.52	2.26	2.41	0.40
79	1,2,3-Trimethoxybenzene	–	1.94	–	–
80	2-tert-Butyl-4-(hydroxtmethyl)-5-formylfuran	–	2.05	3.36	–
81	1,2-Benzenediol, 3-methoxy-	0.32	–	–	–
82	Benzaldehyde, 4-hydroxy-3-methoxy-	0.58	–	–	–
83	Eugenol	2.74	–	–	2.38
84	Benzoic acid, 4-hydroxy-3-methoxy-	2.35	–	2.42	2.26
85	3-Furancarboxylic acid, 5-ethyl-2, 4-dimethyl-, methyl ester	2.96	–	–	2.84
86	Homovanillyl alcohol	–	–	0.76	0.76
87	1,4-Dihydrophenanthrene	–	–	–	1.30
88	Vanillone, aceto-	0.33	–	–	–
89	4-Amino-2,3-xylenol	1.03	–	–	–
90	4,11-Dioxa-3,5-dimethyltetracycloundecane cage compound	1.74	–	1.30	–
91	1-(2,5-Dimethoxyphenyl)-propanol	0.54	–	–	–
92	Phenol, 2,6-dimethoxy-4-(2-propenyl)-	0.88	–	1.37	2.12
93	1(2H)-Naphthalenone, octahydro-5,5,8a-trimethyl-, (4AS-trans)-	1.89	–	–	–
94	Thiophene, 2-isobutyl-5-isopentyl-	–	–	–	0.48
95	Pyrido[1,2-a]benzimidazole, 8-fluoro-	0.34	–	–	
96	1-Butanone, 1-(2,4,6-trihydroxy-3- methylphenyl)-	0.62	–	–	–
97	1,2-Benzenedicarboxylic acid, mono (2-ethylhexyl) ester	–	–	–	0.72

crack producing carbonaceous solid products. The FT-IR spectrums of bio-chars were similar to each other at the same temperatures. The C – C stretching vibrations between 1350 and 1600 cm^{-1} indicate the presence of aromatics and alkanes. The C – O stretching absorbance peaks observed between 1050 and 1350 cm^{-1} indicate the presence of primary, secondary and tertiary alcohols, phenols, ethers and esters. FT-IR spectrums show that the bio-chars obtained from pyrolysis are mainly composed of aromatic and aliphatic compounds.

FT-IR spectrums of bio-oils obtained at 350 °C and 550 °C are given in Figs. 10 and 11 respectively. The list of the compounds identified by GC–MS is given in Tables 4 and 5 respectively. As seen from Tables 4 and 5, bio-oils contain various types of compounds with different molecular structures and molecular weights which were formed from decompositon of hemicellulose, cellulose and lignin in raw material. The results of GC–MS show that there are differences between non-catalytic and catalytic runs. Number and types of compounds produced at higher temperature (550 °C) were greater than at lower temperature (350 °C) which evidences that the decomposition of lignin was not complete and continued as the temperature was further increased.

Bio-oils identified by GC–MS are consisted of complex mixtures of organic compounds from wide variety of chemical groups. These compounds can be grouped into four different classes of monoaromatics, aliphatics, oxygenated compounds, nitrogenated compounds, aromatic compounds and derivatives. Monoaromatics include benzene and derivatives, toluene, furans, phenols and derivatives. Aliphatics are mainly composed of alkanes, alkenes and their derivatives while oxygenated compounds contain aldehydes, ketones, esters and carboxylic acids. Amines and amides such as pyridine, pyrazine and imidazole are classified as nitrogenated compounds. Lastly, polycylic aromatic compounds such as naphthalene phenanthrene and indene were identified by GC–MS analysis.

In accordance with the previous studies reported in literature [60–64] most of the identified compounds in bio-oils were phenolic compounds and their derivatives which were formed by degradation of lignin in the raw material. They consist of phenols, methoxy phenols, alkyl phenols and eugenol. As bio-oils obtained by pyrolysis can be used not only as a fuel in engines or boilers, but also as a valuable organic chemicals, phenols could be considered as one of them for its commercial value. Bio-oils are composed of mainly aldehydes, ketones and phenolic compounds. Most of these compounds are formed from the degradation of lignin and the others are from cellulose. The most abundant compounds in the bio-oils are phenol, cresols, 2,6-dimethoxy phenol, guaiacol, eugenol, 2-cyclopenten-1-one 2-hydroxy-3-methyl- and furan derivatives. During pyrolysis of lignocellulosic biomass, hemicelluloses decompose first (200–280 °C) forming the acidic compounds such as formic and acetic acid. On the other hand, decomposition of cellulose (240–350 °C) produces levoglucosan as a primary breakdown product during thermal treatment, but other anhydroglucoses, furan and furan derivatives are also produced. Phenols and derivatives such as 2,6-dimethoxy phenol, guaiacol and cresols, the majority of the compounds in bio-oils, are obviously the primary products of degradation of lignin (280–500 °C) during pyrolysis [65].

The FT-IR spectrums confirm and are consistent with the list of compounds in Tables 4 and 5. The band intensities show that the most abundant chemical bonds in bio-oils are O – H, C – H, C – O and C═O. Absorbance peaks of the O – H vibrations between 3200 and 3400 cm^{-1} indicate the presence of the abundant compounds of phenols and alcohols and the absorbance peaks of C – H and ═C – H vibrations between 2800 and 3000 cm^{-1} show the presence of alkanes and alkenes. The typical carbonyl group (C═O) streching vibrations between 1700 and 1720 cm^{-1} in bio-oils shows that aldehydes, ketones or carboxylic acids were produced by degradation of raw material. Presence of alcohols and esters is confirmed by C – H bending vibrations between 900 and 1300 cm^{-1} and strong C – O stretching vibrations between 1200 and 1300 cm^{-1} in bio-oils. The C – H deformation vibrations between 1350 and 1450 cm^{-1} indicate the presence of functional groups, – CH, $-CH_2$ and $-CH_3$, characteristic for alkane groups in bio-oils. Aromatic compounds are confirmed by the aromatic C═C stretching vibrations between 1450 and 1550 cm^{-1}. Benzene derivatives and phenol compounds are formed from decomposition of lignin while alkanes, aldehydes, alcohols, carboxylic acids, furans and derivatives are originated from hemicelluloses and cellulose [66,67].

4. Conclusion

In this study, pyrolysis of a specific biomass, *E. spectabilis*, was carried out in a fixed-bed reactor with and without catalyst to obtain solid (biochar) and liquid (bio-oil) products. The effects of pyrolysis parameters including temperature, heating rate, particle size and sweeping gas

flow rate were investigated on product yields. The experimental data showed that the highest yield (34.62%) of bio-oil was obtained at 500 °C with heating rate of 50 °C/min when 0.224 > Dp > 0.150 mm particle size raw material and 100 mL/min of sweeping gas flow rate were used in the non-catalytic runs. Applicability of three boron minerals (tincal, colemanite and ulexite) as catalyst in the pyrolysis process was also investigated and it was found that catalysts have changed both distribution and composition of produced liquids. Ulexite has proven to have greater effect than others in improving quantity and quality of produced bio-oils. Besides, the effects of particle size and sweeping gas flow rate on product yields were also determined under the optimum temperature and heating rate conditions.

The composition of the bio-oils was characterized by chromatographic and spectroscopic techniques as well as the calorific values of bio-chars and bio-oils. The bio-oils were found to be highly heterogeneous complex mixtures of monoaromatics, polyaromatics aliphatics, oxygenated and nitrogenated organic compounds. The FT-IR analysis showed that the composition of bio-oils was dominated by phenolics and oxygenated compounds. The produced bio-oils had higher calorific values than the raw material. The GC–MS results of bio-oils indicate that *E. spectabilis* can be a promising candidate for renewable fuel production or high value chemicals.

References

[1] E.A. Varol, B.B. Uzun, E. Önal, A.E. Pütün, Synthetic fuel production from cottonseed: fast pyrolysis and a TGA/FT-IR/MS study, Journal of Analytical and Applied Pyrolysis 105 (2014) 83–90.
[2] H.L. Chum, R.P. Overend, Biomass and renewable fuels, Fuel Processing Technology 71 (2001) 187–195.
[3] A.V. Brigdwater, Review of fast pyrolysis of biomass and product upgrading, Biomass and Bioenergy 38 (2012) 68–94.
[4] G.W. Huber, S. Iborra, A. Corma, Synthesis of transportation fuels from biomass: chemistry, catalysts, and engineering, Chemical Reviews 106 (2006) 4044–4098.
[5] T. Aysu, M.M. Küçük, Biomass pyrolysis in a fixed-bed reactor: effects of pyrolysis parameters on product yields and characterization of products, Energy 64 (2014) 1002–1025.
[6] A. Demirbaş, Biomass resource facilities and biomass conversion processing for fuels and chemicals, Energy Conversion and Management 42 (2001) 1357–1378.
[7] Q. Lu, L. Wenzhi, Z. Xifeng, Overview of fuel properties of biomass fast pyrolysis oils, Energy Conversion and Management 50 (2009) 1376–1383.
[8] Z. Leiyu, Y. Hongmin, W. Hao, W. Meng, C. Daqian, Catalytic pyrolysis of rice husk by mixing with zinc oxide: characterization of bio-oil and its rheological behaviour, Fuel Processing Technology 106 (2013) 385–391.
[9] Q. Zhang, J. Chang, T. Wang, Y. Xu, Review of biomass pyrolysis oil properties and upgrading research, Energy Conversion and Management 48 (2007) 87–92.
[10] M.I. Nokkosmaki, E.T. Kuoppala, E.A. Leppamaki, A.O.I. Krause, Catalytic conversion of biomass pyrolysis vapours with zinc oxide, Journal of Analytical and Applied Pyrolysis 55 (2000) 119–131.
[11] K. Tekin, S. Karagöz, S. Bektaş, Hydrothermal liquefaction of beech wood using a natural calcium borate mineral, Journal of Supercritical Fluids 72 (2012) 134–139.
[12] K.P. Shadangi, K. Mohanty, Production and characterization of pyrolytic oil by catalytic pyrolysis of Niger seed, Fuel 126 (2014) 109–115.
[13] T. Aysu, M.M. Küçük, The liquefaction of *Heracleum persicum* by supercritical fluid extraction, Energy Sources, Part A: Recovery, Utilization, and Environmental Effects 35 (2013) 1787–1795.
[14] C. Li, J.G. Shi, Y.P. Zhang, C.Z. Zhang, Constituents of *Eremurus chinensis*, Journal of Natural Products 63 (2000) 653–656.
[15] M. Tosun, S. Ercisli, H. Ozer, M. Turan, T. Polat, E. Ozturk, H. Padem, H. Kılıcgun, Chemical composition and antioxidant activity of foxtail lily (*Eremurus spectabilis*), Acta Scientiarum Polonorum-Hortorum Cultus 11 (2012) 145–153.
[16] T. Baytop, Therapy with Medicinal Plants in Turkey (Past and Present), 2nd ed. Nobel Medicine Publication, İstanbul, 1999. 118–119.
[17] E. Tuzlacı, Çiriş plants of Turkey (I), Journal of Pharmaceutical of Marmara University 12 (1985) 91–100.
[18] T. Taskin, L. Bitis, A.S.B. Tan, Antioxidant and antimicrobial activities of different extracts from *Eremurus spectabilis* leaves, Spatula DD 2 (2012) 213–217.
[19] Tappi Test Methods, Tappi Press, Atlanta, Georgia, 1998.
[20] L.E. Wise, E.C. John, Wood Chemistry, Second ed. Reinhold Publishing, New York, 1952.
[21] Y.J. Qian, C.J. Zuo, J. Tan, J.H. He, Structural analysis of bio-oils from sub- and supercritical water liquefaction of woody biomass, Energy 32 (2007) 196–202.
[22] L. García, M.L. Salvador, J. Arauzo, R. Bilbao, Catalytic pyrolysis of biomass: influence of the catalyst pretreatment on gas yields, Journal of Analytical and Applied Pyrolysis 58–59 (2001) 491–501.
[23] E. Antonakou, A. Lappas, M.H. Nilsen, A. Bouzga, M. Stöcker, Evaluation of various types of AL-MCM-41 materials as catalysts in biomass pyrolysis for the production of bio-fuels and chemicals, Fuel 85 (2006) 2202–2212.
[24] Z.G. Liu, F.S. Zhang, Effects of various solvents on the liquefaction of biomass to the liquefaction of biomass to produce fuels and chemical feedstocks, Energy Conversion and Management 49 (2008) 3498–3504.
[25] T. Fisher, N. Hajaligol, B. Waymack, D. Kellogg, Pyrolysis behavior and kinetics of biomass derived materials, Journal of Analytical and Applied Pyrolysis 62 (2002) 331–349.
[26] W. Jennings, T. Shibamoto, Qualitative Analysis of Flavor and Fragrance Volatiles by Glass Capillary Gas Chromatography, Academic Press, New York, 1980.
[27] R.P. Adams, Identification of Essential Oil Components by Gas Chromatograph Quadrupole Mass Spectroscopy, Allured Publishing Corporation, Carol Stream, USA, 2001.
[28] L. Fagbemi, L. Khezami, R. Capart, Pyrolysis products from different biomasses: application to the thermal cracking of tar, Applied Energy 69 (2001) 293–306.
[29] M.R. Rover, P.A. Johnston, L.E. Whitmer, R.G. Smith, R.C. Brown, The effect of pyrolysis temperature on recovery of bio-oil as distinctive stage fractions, Journal of Analytical and Applied Pyrolysis 105 (2014) 262–268.
[30] E. Önal, B.B. Uzun, A.E. Pütün, Bio-oil production via co-pyrolysis of almond shell as biomass and high density polyethylene, Energy Conversion and Management 78 (2014) 704–710.
[31] R. Azargohar, S. Nanda, J.A. Kozinski, A.K. Dalai, R. Sutarto, Effects of temperature on the physicochemical characteristics of fast pyrolysis bio-chars derived from Canadian waste biomass, Fuel 125 (2014) 90–100.
[32] J.F. Peters, F. Petrakopoulou, J. Dufour, Exergetic analysis of a fast pyrolysis process for bio-oil production, Fuel Processing Technology 119 (2014) 245–255.
[33] M.C.C. Maguyon, S.C. Capareda, Evaluating the effects of temperature on pressurized pyrolysis of *Nannochloropsis oculata* based on products yields and characteristics, Energy Conversion and Management 76 (2013) 764–773.
[34] K.P. Shadangi, K. Mohanty, Thermal and catalytic pyrolysis of Karanja seed to produce liquid fuel, Fuel 115 (2014) 434–442.
[35] P.T. Williams, A.R. Reed, Pre-formed activated carbon matting derived from the pyrolysis of biomass natural fibre textile waste, Journal of Analytical and Applied Pyrolysis 70 (2003) 563–577.
[36] S. Şensöz, D. Angın, Pyrolysis of safflower (*Charthamus tinctorius* L.) seed pres cake: part 1. The effects of pyrolysis parameters on the product yields, Bioresource Technology 99 (2008) 5492–5497.
[37] L. Li, H. Zhang, Production and characterization of pyrolysis oil from Herbaceous biomass (*Achnatherum splendens*), Energy Sources 27 (2005) 319–326.
[38] R. Zanzi, K. Sjöström, E. Björnbom, Rapid pyrolysis of agricultural residues at high temperatures, Biomass and Bioenergy 23 (2002) 357–366.
[39] A. Demirbaş, Determination of calorific values of bio-chars and pyro-oils from pyrolysis of beech trunkbarks, Journal of Analytical and Applied Pyrolysis 72 (2004) 215–219.
[40] J.M. Encinar, J.F. Gonzalez, Fixed-bed pyrolysis of *Cynara carduncules* L. product yields and compositions, Fuel Processing Technology 68 (2000) 209–222.
[41] R.J.M. Westerhof, H.S. Nygard, W.P.M. Van Swaaij, S.R.A. Kersten, D.W.F. Brilman, Effect of particle geometry and microstructure on fast pyrolysis of beech wood, Energy & Fuels 26 (2012) 2274–2280.
[42] Ö.M. Koçkar, Ö. Onay, A.E. Pütün, E. Pütün, Fixed-bed pyrolysis of hazelnut shell: a study on mass transfer limitations on product yields and characterization of the pyrolysis oil, Energy Sources 22 (2000) 913–924.
[43] B.B. Uzun, A.E. Pütün, E. Pütün, Rapid pyrolysis of olive residue. 1. Effect of heat and mass transfer limitations on product yields and bio-oil compositions, Energy & Fuels 21 (2007) 1768–1776.
[44] J. Shen, X.S. Wang, M.G. Perez, D. Mourant, M.J. Rhodes, C.Z. Li, Effects of particle size on the fast pyrolysis of oil mallee woody biomass, Fuel 88 (2009) 1810–1817.
[45] S. Zhou, M.G. Perez, B. Pecha, A.G. McDonald, R.J.M. Westerhof, Effect of particle size on the composition of lignin derived oligomers obtained by fast pyrolysis of beech wood, Fuel 125 (2014) 15–19.
[46] E. Harfi, A. Mokhlisse, M.B. Chanaa, Effect of water vapor on the pyrolysis of the Moroccan (Tarfaya) oil shale, Journal of Analytical and Applied Pyrolysis 48 (1999) 65–76.
[47] H.F. Gerçel, The effect of a sweeping gas flow rate on the fast pyrolysis of biomass, Energy Sources 24 (2002) 633–642.
[48] K. Açıkalın, F. Karaca, E. Bolat, Pyrolysis of pistachio shell: effects of pyrolysis conditions and analysis of products, Fuel 95 (2012) 169–177.
[49] A.R. Mohamed, Z. Hamzah, M.Z.M. Daud, Z. Zakaria, The effects of holding time and the sweeping nitrogen gas flowrates on the pyrolysis of EFB using a fixed bed reactor, Procedia Engineering 53 (2013) 185–191.
[50] M. Auta, L.M. Ern, B.H. Hameed, Fixed-bed catalytic and non-catalytic empty fruit bunch biomass pyrolysis, Journal of Analytical and Applied Pyrolysis 107 (2014) 67–72.
[51] A. Veses, M. Aznar, I. Martínez, J.D. Martínez, J.M. López, M.V. Navarro, M.S. Callén, R. Murillo, T. García, Catalytic pyrolysis of wood biomass in an auger reactor using calcium-based catalysts, Bioresource Technology 162 (2014) 250–258.
[52] B. Li, W. Lv, Q. Zhang, T. Wang, L. Ma, Pyrolysis and catalytic upgrading of pine wood in a combination of auger reactor and fixed bed, Fuel 129 (2014) 61–67.
[53] J. Jae, R. Coolman, T.J. Mountziaris, G.W. Huber, Catalytic fast pyrolysis of lignocellulosic biomass in a process development unit with continual catalyst addition and removal, Chemical Engineering Science 108 (2014) 33–46.
[54] M.S. AbuBakar, J.O. Titiloye, Catalytic pyrolysis of rice husk for bio-oil production, Journal of Analytical and Applied Pyrolysis 103 (2013) 362–368.
[55] J. Han, X. Wang, J. Yue, S. Gao, G. Xu, Catalytic upgrading of coal pyrolysis tar over char-based catalysts, Fuel Processing Technology 122 (2014) 98–106.
[56] S.R. Naqvi, Y. Uemura, S.B. Yusup, Catalytic pyrolysis of paddy husk in a drop type pyrolyzer for bio-oil production: the role of temperature and catalyst, Journal of Analytical and Applied Pyrolysis 106 (2014) 57–62.
[57] J. Shao, R. Yan, H. Chen, H. Yang, D.H. Lee, Catalytic effect of metal oxides on pyrolysis of sewage sludge, Fuel Processing Technology 91 (2010) 1113–1118.

[58] D. Guo, S. Wu, B. Liu, X. Yin, Q. Yang, Catalytic effects of NaOH and Na_2CO_3 additives on alkali lignin pyrolysis and gasification, Applied Energy 95 (2012) 22–30.
[59] K. Tekin, M.K. Akalın, S. Bektaş, S. Karagöz, Hydrothermal wood processing using borax decahydrate and sodium borohydride, Journal of Analytical and Applied Pyrolysis 104 (2013) 68–72.
[60] M.S.A. Moraes, F. Georges, S.R. Almeida, F.C. Damasceno, G.P.S. Maciel, C.A. Zini, R.A. Jacques, E.B. Caramão, Analysis of products from pyrolysis of Brazilian sugar cane straw, Fuel Processing Technology 101 (2012) 35–43.
[61] I.H. Hwang, J. Kobayashi, K. Kawamoto, Characterization of products obtained from pyrolysis and steam gasification of wood waste, RDF, and RPF, Waste Management 34 (2014) 402–410.
[62] J.D. Martínez, A. Veses, A.M. Mastral, R. Murillo, M.V. Navarro, N. Puy, A. Artigues, J. Bartrolí, T. García, Co-pyrolysis of biomass with waste tyres: upgrading of liquid biofuel, Fuel Processing Technology 119 (2014) 263–271.
[63] E. Parparita, M. Brebu, Md.A. Uddin, J. Yanik, C. Vasile, Pyrolysis behaviors of various biomasses, Polymer Degradation and Stability 100 (2014) 1–9.
[64] C. Peng, G. Zhang, J. Yue, G. Xu, Pyrolysis of lignin for phenols with alkaline additive, Fuel Processing Technology 124 (2014) 212–221.
[65] C.A.S. Hill, Wood Modification Chemical, Thermal and Other Processes, John Wiley & Sons Ltd, The Atrium, Southern Gate, Chichester, West Sussex PO19 8SQ, England, 2007.
[66] V. Gomez-Serrano, F. Piriz-Almeida, C.J. Duran-Valle, J. Pastor-Villegas, Formation of oxygen structures by air activation. A study by FT-IR spectroscopy, Carbon 37 (1999) 1517–1528.
[67] İ. Demiral, Ş.Ç. Kul, Pyrolysis of apricot kernel shell in a fixed-bed reactor: characterization of bio-oil and char, Journal of Analytical and Applied Pyrolysis 107 (2014) 17–24.